



HAL
open science

Morphological features of tooth development and replacement in the rabbit *Oryctolagus cuniculus*

Ludivine Bertonnier-Brouty, Laurent Viriot, Thierry Joly, Cyril Charles

► To cite this version:

Ludivine Bertonnier-Brouty, Laurent Viriot, Thierry Joly, Cyril Charles. Morphological features of tooth development and replacement in the rabbit *Oryctolagus cuniculus*. *Archives of Oral Biology*, 2020, 109, pp.104576. 10.1016/j.archoralbio.2019.104576 . hal-03488382

HAL Id: hal-03488382

<https://hal.science/hal-03488382v1>

Submitted on 21 Dec 2021

HAL is a multi-disciplinary open access archive for the deposit and dissemination of scientific research documents, whether they are published or not. The documents may come from teaching and research institutions in France or abroad, or from public or private research centers.

L'archive ouverte pluridisciplinaire **HAL**, est destinée au dépôt et à la diffusion de documents scientifiques de niveau recherche, publiés ou non, émanant des établissements d'enseignement et de recherche français ou étrangers, des laboratoires publics ou privés.



Distributed under a Creative Commons Attribution - NonCommercial 4.0 International License

1 **Title page**

2

3 Title: Morphological features of tooth development and replacement in the rabbit *Oryctolagus*
4 *cuniculus*

5

6 Authors: Ludivine Bertonnier-Brouty^{1*}, Laurent Viriot¹, Thierry Joly^{2, 3}, Cyril Charles¹

7

8 ¹ Institut de Génomique Fonctionnelle de Lyon, Université de Lyon, CNRS UMR 5242, Ecole
9 Normale Supérieure de Lyon, Université Claude Bernard Lyon 1, Lyon, France

10 ² ISARA-Lyon, F-69007 Lyon, France

11 ³ VetAgroSup, UPSP ICE, F-69280 Marcy l'Etoile, France

12 * Corresponding author: Ludivine.bertonnierbrouty@ens-lyon.fr

13

14 **Highlights**

- 15 • Tooth replacement is initiated at the lingual side of the deciduous tooth
- 16 • Permanent tooth morphogenesis can occur at the vestibular side of the deciduous tooth
- 17 • Rabbit first molars present a rudimentary successional dental lamina
- 18 • Newborn rabbits present dentin holes in their incisors opening the pulp cavity
- 19 • The rabbit is a suitable model to study mammalian tooth replacement

20

21 **Abstract**

22 Dental development mechanisms in mammals are highly studied using the mouse as a
23 biological model. However, the mouse has a single, unreplaced, set of teeth. Features of
24 mammalian tooth replacement are thus poorly known. In this paper, we study mammalian
25 tooth development and replacement using the European rabbit, *Oryctolagus cuniculus*, as a

26 new model. Using 3D-reconstructions associated with histological sections, we obtained the
27 complete description of the histo-morphological chronology of dental development and
28 replacement in rabbit. We also describe the presence of holes in the dentin opening the pulpal
29 cavity in newborns. These holes are quickly repaired with a new and fast apposition of dentin
30 from the pre-existing odontoblasts. The detailed dental morphogenesis chronology presented
31 allows us to propose the rabbit *Oryctolagus cuniculus* as a suitable model to study
32 mammalian tooth replacement

33 **Keywords**

34 Tooth development, mammalian tooth replacement, diphyodonty, 3D-reconstructions, rabbit
35 teeth

36

37 **Main text**

38 **Introduction**

39 The signaling pathways involved in tooth development and morphogenesis are highly
40 studied in mice (Balic & Thesleff, 2015), fishes (Rasch et al., 2016), or reptiles (Whitlock &
41 Richman, 2013). Regarding tooth replacement (Bertin, Thivichon-Prince, LeBlanc, Caldwell,
42 & Viriot, 2018), a majority of fish and reptiles have the ability to replace their teeth
43 continuously throughout their life (polyphyodonty) contrary to the majority of mammals that
44 replace their teeth only once (diphyodonty). In mammals, most odontogenesis studies use the
45 mouse as a model species and mouse tooth development is well described from its
46 morphogenesis to the genetic mechanisms involved. Tooth development is commonly divided
47 into five stages: the placode, the bud, the cap, the bell, and finally the maturation stages. At
48 first, a dental placode appears from the oral epithelium by thickening. Next, at the bud stage,
49 the dental epithelium invaginates, followed by a condensation of the dental mesenchyme.
50 Then, the epithelium starts to fold, forming the cap stage; this stage marks the beginning of

51 histo-differentiation. The tooth cuspidogenesis starts at the bell stage. Cells begin to secrete
52 dentin and enamel layers at the late bell stage. In the maturation stage, the tooth gets fully
53 mineralized. Because the mouse has no dental replacement, the mechanisms of tooth
54 replacement in mammals are poorly known. Some studies have been done in the ferret
55 (Järvinen, Tummers, & Thesleff, 2009; Jussila, Crespo Yanez, & Thesleff, 2014), the shrew
56 (Järvinen, Välimäki, Pummila, Thesleff, & Jernvall, 2008), the fruit bat (Popa, Anthwal, &
57 Tucker, 2016) and the minipig (Wang et al., 2014; Wang et al., 2019). Altogether, these
58 studies have characterized the morphological changes involved in tooth replacement: the
59 initiation of tooth replacement begins by a budding of the replacement dental lamina at the
60 lingual part of the tooth stalk. Then the replacement dental lamina plunges into the
61 mesenchyme and the tooth morphogenesis begins. Moreover, the first molecular observations
62 of tooth replacement mechanisms in mammals have been done in the ferret *Mustela putorius*
63 *furo* (Järvinen et al., 2009; Jussila et al., 2014). However, few developmental stages were
64 studied due to the difficulty to obtain ferret embryos at the correct stage and the presence of
65 seasonal estrus. The shrew *Sorex araneus* is limited as a model because their deciduous teeth
66 never erupt. In the fruit bat *Eidolon helvum*, 3D reconstructions and histological sections are
67 good illustrations of mammalian tooth replacement but authors indicated that this species is
68 no longer available for experimental purposes (Popa et al., 2016). Tooth development and
69 replacement has also been described in the minipig *Sus scrofa*, whose teeth size and
70 morphology are pretty similar to human teeth (Wang et al. 2014). However, at least 100 days
71 are necessary from the appearance of the replacement dental lamina to the mineralization of
72 the replacement tooth in the minipig. So, the slow development, the size of the animal and
73 ethical concerns are significant obstacles to study tooth development in the minipig. For now,
74 any model can answer both morphological and molecular questions about mammalian tooth
75 replacement, and previous studies are restricted to some parts of dental development. We thus

76 decided to use the European rabbit (*Oryctolagus cuniculus*) as a new model to study tooth
77 development and replacement. The rabbit is already an important model for biomedical
78 research (Bosze & Houdebine, 2006) and the whole genome has been sequenced (OryCun2.0,
79 2009). The rabbit dentition is diphyodont with a replacement of some incisors and all
80 premolars (Horowitz, Weisbroth, & Scher, 1973). They possess two upper and one lower
81 incisors, three upper and two lower premolars and three upper and lower molars on each side.
82 Deciduous premolars have a limited growth with root formation whereas permanent teeth are
83 continuously growing (Sych & Reade, 1987). Associated with this continuous growth, each
84 permanent tooth in the rabbit is supposed to possess a pool of mesenchymal and epithelial
85 stem cells in its growing part, as in all hypselodont species (Tummers & Thesleff, 2003).
86 Rabbit dental development has been studied during the 70's and 80's, Horowitz and
87 collaborators (1973) completing a chronology of deciduous tooth eruption using radiography,
88 giving information on the mineralized part of the teeth. Navarro carried out histological
89 studies of the postnatal development in maxillary (1975) and mandibular cheek teeth (1976).
90 However, the deciduous incisors and premolars are completely mineralized at birth and thus
91 Navarro et al. do not document their development. Hirschfeld et al. (1973) and Ooë (1980)
92 have studied the incisor development in embryos, but nothing has been reported for the cheek
93 teeth development. Michaeli et al., (1980) gave a simplified chronology of rabbit cheek tooth
94 development during embryogenesis without separating each tooth and with histological
95 illustrations only for the post-natal stages. All these studies result in a composite and
96 fragmental chronology of the tooth development in rabbit. The purpose of our work is to
97 supply a complete report of the development of all deciduous and permanent teeth in the
98 rabbit. We decided to study rabbits from 12 days post fertilization to 4 days post-natal in order
99 to obtain a complete chronology of tooth development from the initiation of the deciduous
100 tooth to the mineralization of the replacement teeth. Using histological studies and 3D-

101 reconstruction of soft tissues, we present the developmental and morphological characteristics
102 of rabbit teeth.

103

104 **Material & Method**

105 *Samples*

106 Embryos and newborn rabbit samples used for histology and X-Ray microtomography
107 were obtained through collaboration with a standard production for feeding recorded at the
108 Biology Departmental livestock establishment (EDE) n°38044102. We worked on common
109 rabbit breeding regularly crossed with wild rabbits to ensure genetic mixing. The gestation
110 period for a rabbit is about 31 days. We collected embryos at 12, 14, 16, 18, 20, 22, 24, 26
111 and 28 days post fertilization (dpf) and rabbits at 0, 1, 2, 3 and 4 days post-natal (dpm). 3 to 21
112 embryos were analyzed for each developmental stage. For juvenile and adult rabbits,
113 observations were made on 230 specimens of *Oryctolagus cuniculus* from the Muséum
114 National d'Histoire Naturelle (MNHN, Paris, France). Age of the specimens were not
115 indicated so we used the skull size as proxy, our sampling contained skull size from 36.65 to
116 108.8mm. In the 230 specimens, only four still had their deciduous teeth. Each tooth is
117 specifically named: we use 'I', 'P' and 'M' for incisor, premolar and molar respectively; the
118 deciduous teeth are indicated with a 'd'; the tooth number is in exponent for the upper teeth
119 and in index for the lower teeth.

120

121 *Histology*

122 After dissection of the upper and lower jaws, samples were fixed overnight in 4%
123 PFA. Samples were then rehydrated and fixed in Holland Bouin solution during 1 day. Jaws
124 were demineralized for 1 to 7 days in Morse's solution (10% sodium citrate + 22% formic
125 acid) or in RNase-free 12.5% EDTA + 2.5% PFA during 6 weeks, according to the

126 subsequent experiment to be performed. Then, jaws were embedded in paraffin and serially
127 sectioned with a Leica microtome (7 μ m thick slices). Sections were carried out in parasagittal
128 or frontal plane. For histological purpose, samples were dewaxed in xylene, and then colored
129 via an optimized Masson's trichrome protocol with aniline blue, hemalum and fuschin.

130

131 *In situ hybridization*

132 Specific probes for Osteocalcin and K14 have been designed using the rabbit genome
133 available online (OryCun2.0, 2009). Each probe has been sequenced before use, and then
134 probes were synthesized with RNA-dig labeling nucleotides. Classical mouse in situ protocol
135 has been optimized to be compatible with rabbit tissues. Tissues were treated with HCl 0.2M,
136 with proteinase K 5 μ g/ml and then incubated with TEA-Acetic anhydride. Hybridization step
137 were done at 62°C. Sections were whashed in a warm washing buffer (1X SSC and 50%
138 formamide) and in MABT solution. After 2 hours in a blocking solution, slides were covered
139 of anti-Dig-AP-antibody solution at 4°C overnight. Sections were washed with MABT and
140 NTMT with teramisol. Sections were stained with BM purple solution and mounted in
141 Aquatex.

142

143 *X-ray microtomography and 3D reconstruction*

144 Conventional X-ray microtomography allows reconstructing 3D models of
145 mineralized tissues such as bony head and teeth, thus providing a non-invasive access to
146 internal structures. Using phosphotungstic acid (PTA) staining, that binds heavily to various
147 proteins and connective tissue (Metscher, 2009); we were able to detect soft tissues by X-Ray
148 microtomography. After fixation, half-head samples were stained in a solution 0.3% PTA in
149 70% ethanol between 1 week and 8 months according to the size of the sample. Oldest
150 specimens were demineralized to better detect the soft tissue staining. Once the PTA contrast

151 staining was complete, samples were embedded in paraffin and radiographed using a Phoenix
152 Nanotom S (GE Measurement and Control), which was set up with a tungsten source X-ray
153 tube operating at 100 kV and 70 μ A for the mineralized tissues and 60kV and 70 μ A for the
154 soft tissues. The Phoenix datosx2CT software was applied to gather radiographies in a
155 reconstructed 3D volume, in which the voxel size ranged from 1 to 12 μ m depending on the
156 size of the specimen. Post-treatment of 3D volumes, including virtual sectioning as well as
157 sub-volume extractions, was performed using VG-studio max software. Surface smoothing
158 was done with Meshlab software. Incisors hole positions were detected using VG-studio max
159 software and frontal sections were done at each hole using a rotation section plane to respect
160 the natural curvature plane of the incisors. We studied 59 holes from ten incisors (6
161 individuals); the two remaining incisors were used for histology purposes. The centroid of the
162 incisor section was drawn using ImageJ software and mesio-distal and linguo-vestibular axes
163 were positioned in the incisor section. An angle was calculated to determine the hole position,
164 with the mesial position at 0° (and 360°), the vestibular at 90°, the distal at 180° and the
165 lingual position at 270°. Plots were made using R software and the ggplot2 library.

166

167 **Results**

168 *Chronology of incisor development and replacement*

169 We have observed the establishment of the incisors on the upper and lower jaws. The
170 dI1 and the dI2 incisors in the upper and lower jaws appear synchronous in their development.
171 Rabbits have another incisor in the maxillary, named the dI³, which is replaced during
172 ontogeny. We will focus here on the description of the upper incisors (Fig.1), since we do not
173 observe dental replacement in the lower ones. All our 3D reconstructions of the epithelial
174 parts of the incisors are available in Morphomuseum (3D Dataset will remain locked until
175 publication of the main article, Bertonnier-Brouty, Viriot, Joly, & Charles, 2019).

176

177 At 12 dpf, we observed no morphological structure of incisor development. Then, at
178 14 dpf, we detect the initiation of the placode formation at the upper and lower jaws (Fig.1).
179 The epithelium is thicker and the mesenchyme begins to condensate around it. At this stage,
180 right and left placodes are not connected to each other. Two days later, it is still impossible to
181 name the incisors, the lower and upper incisors are at the bud stage, the left and right buds
182 seem now connected lingually. At 18 dpf, all the upper incisors are linked to each other and to
183 the oral epithelium by an epithelium bond, supposed to be a dental lamina rest. As the three
184 incisors follow each other in a mesio-distal plane they are identifiable. From this stage, we
185 can follow the development of each tooth individually.

186

187 Vestigial incisor dI^1

188 At 18 dpf, the first upper incisor is already mineralized with dentin surrounded by
189 dental soft tissues very close to the oral epithelium. This dI^1 is a vestigial tooth; it will not
190 give rise to a functional incisor (Fig.2, A). At 24 dpf, the dI^1 has passed through the oral
191 epithelium and is now trapped in the oral mucosa (blue triangle in Fig.1, Fig.S1). At 28 dpf,
192 the dI^1 is shed.

193

194 dI^2

195 At 18 dpf, the dI^2 is at the cap stage, linked mesially to the other dI^2 and in rotation. As in
196 mouse (Mucchielli & Mitsiadis, 2000), the dI^2 rotates antero-posteriorly and become parallel
197 to the long axis of the jaws, contrary to molars that stay perpendicular to the jaw axis (Fig.1).
198 At 20 dpf, the dental lamina that links the teeth together is completely disorganized and the
199 two dI^2 are no longer linked. The dI^2 has already secreted a thin layer of dentin and the 3D
200 reconstructions show that the vestibular and lingual cervical loops are well formed. These

201 structures are supposed to contain the stem cells that will allow the continuous growth of the
202 tooth during the animal's entire life. At 22 dpf, the teeth are completely separated. At 24 dpf,
203 the dI^2 occlusal surface is very close to the oral epithelium and highly mineralized. The dI^2
204 presents enamel in its entire mineralized surface. We observed a big cervical loop at the
205 vestibular side and a very small one at the lingual part and this incisor has a fold on its
206 vestibular surface on the mesial side. At 26 dpf, the dI^2 is close to erupt. The secretion of
207 enamel at the vestibular and lingual part of the tooth continues. At 28 dpf, the dI^2 is erupting.
208 At birth, the unworn dI^2 presents enamel in the entire erupted occlusal surface. In direction to
209 the growth zone, we detect enamel in the vestibular and the lingual part, and then the enamel
210 production in the lingual part stops and enamel is secreted only in the vestibular part of the
211 tooth. At 4 dpn, the dI^2 are worn in their occlusal surface, showing the dentin. In the juvenile,
212 around 1 month post-natal, we observed that the dI^2 present enamel only in the vestibular
213 surface, so the entire part with enamel in the lingual and vestibular position is already worn
214 (Fig.2, A). In adult, the dI^2 is ever-growing. We observed that the dI^2 and the I^3 do not have
215 the same shape at the occlusal surface, the dI^2 has a sharper beveled edge form compared to
216 the I^3 , linked to the gnaw ability of the dI^2 .

217

218 dI^3

219 At 18 dpf, we observed the dI^3 in a transitional stage between bud and cap at the distal
220 position of the dI^2 . At the vestibular part of the dI^3 , we observed an epithelium structure
221 distally oriented that is probably a dental lamina rest (Fig.1, pink triangle). At 20 dpf, the dI^3 ,
222 still connected to the dI^2 , is now in a cap stage and rotates antero-posteriorly. At 22 dpf, dI^3 is
223 still linked to the oral epithelium but separated to the dI^2 . We observed a lingual budding of
224 the replacement dental lamina in the dI^3 (Fig.1, black triangle). At 24 dpf, the dI^3 is already
225 well mineralized and now perfectly orientated compared to the working position. The dI^3

226 presents small cervical loops at the vestibular and lingual part of the tooth. We detect the
227 replacement dental lamina of the dI^3 attached to the antero-lingual part of the tooth, already
228 parallel to the oral epithelium. At 26 dpf, the cervical loops of the dI^3 are reduced; we
229 observed the start of the root formation. The replacement dental lamina has grown but is still
230 linked to the dI^3 . At 28 dpf, the dI^3 has erupted to the oral epithelium but still do not exit of
231 the oral mucosa. The dI^3 is the only incisor that develops roots; the pulpal cavity seems to
232 close. The I^3 is in a bud stage and no longer linked to the dI^3 . At birth, the dI^3 present enamel
233 in the entire occlusal surface. The I^3 continues its development in a cap stage. At 4 dpn, the
234 permanent I^3 begins to mineralize, the roots of the dI^3 are still in mineralization. The dI^3 is
235 worn in the occlusal surface, showing the dentin. In the juvenile, the roots of the dI^3 have
236 finished mineralizing and we observed root resorption. The I^3 is now well mineralized and
237 will soon replace the dI^3 (Fig.2, A). Interestingly, the I^3 is entirely covered by enamel in
238 juveniles on the while the dI^2 have enamel only in the vestibular part of the tooth. In adult, the
239 I^3 is covered by enamel in the vestibular and lingual part of the tooth (Fig.2A, Fig.S2).

240

241 *Specificity of the rabbit incisors: dentin holes in the newborn incisors*

242 The dI^2 incisor mineralizes at 24 dpf, a thin and continuous layer of dentin is secreted
243 by the odontoblasts. Enamel is first secreted in all the surface of the dI^2 , then restricted to the
244 vestibular and lingual sides to finally be secreted only in the vestibular part of the tooth
245 (Fig.S2). In samples from 24 dpf to 28 dpf, the dentin layer of the dI^2 is continuous; no
246 uneven formation of dentin is detected. However, we observed dentin defects in newborn
247 rabbits. In rabbits from 0 to 4 dpn, we detect the presence of holes in the dentin of the dI^2 ,
248 opening the pulpal cavity at specific locations, the lower incisors are not affected (Fig.3, A-D).
249 Older samples, from juveniles to adults, do not have holes in their incisors, indicating a
250 mechanism of tooth repair.

251 To study the appearance and repair of the holes, we identified 59 holes in 10 dI²
252 incisors from six individuals from 0 to 4 dpn. We precisely localized each hole in frontal
253 section of the incisor by calculating an angle in function of the incisor centroid and the mesio-
254 distal and linguo-vestibular planes (Fig.3, A). We observed that the majority of the holes are
255 at the distal side of the tooth (73%), and some in the mesial part (27%). No hole is observed in
256 the vestibular or lingual part of the incisor. By comparing the repartition of the holes in right
257 and left incisors of a same individual, we conclude that holes are independently localized in
258 the two incisors on the proximo-occlusal axis; we did not observe any symmetry (Fig.3, B).
259 Moreover, the number of holes is variable from one tooth to another, even in the same
260 individual. Interestingly, on the 3 and 4 dpn rabbits, we observed a reparation system by the
261 presence of dentin and cells inside the hole (Fig.3, D). This reparation seems very efficient as
262 the holes appear at birth and are repaired two days later. We decided to use *Osteocalcin in situ*
263 staining as a marker for the dentin formation process (Fig.3, E). We observed that the cells in
264 the holes are odontoblasts still expressing *Osteocalcin*, so still in a secretion stage. These
265 secreting odontoblasts, coming from the pre-existing odontoblast layer, could explain the
266 presence of new dentin in the holes. *Keratin 14* staining indicates the epithelial cells; we
267 wanted to check if the holes could deform the layer of epithelial cells. We detect in the incisor
268 a perfect layer of ameloblasts that is not disrupted by the presence of the hole that are formed
269 at the mesial or distal edges of the enamel layer (Fig.3, F).

270 Therefore, these holes are present only in newborns at the mesial or distal limits of the
271 enamel layer, are repaired by the pre-existing odontoblasts and no longer observed during
272 adulthood. Holes seem thus to occur in a very short period of development around or just after
273 the birth of the animal.

274

275

276 *Chronology of cheek teeth development and replacement*

277 We observed the establishment of the cheek teeth on the upper (Fig.4) and lower
278 (Fig.5) jaws. We focus here our description on the mechanisms of tooth replacement. The
279 steps of the tooth replacement are illustrated in the figure indicating all the tooth tissues
280 (Fig.6). All our 3D-reconstructions of the epithelial parts of the cheek teeth are available in
281 Morphomuseum (Bertonnier-Brouty et al., 2019).

282

283 At 12 dpf, the oral epithelium is regular in thickness; we detect no morphological trace
284 of tooth development initiation. Two days later, the oral epithelium has thickened in the upper
285 and lower jaws, forming the dental lamina (Figs.4, 5). The dental lamina thickens
286 continuously over a large part of each mouth quadrant and the mesenchyme seems condensed
287 around it, forming the dental placode. In contrast to humans (Juuri & Balic, 2017), the rabbits
288 do not have a unique continuous dental lamina around the jaw arch but distinct dental laminae
289 for the right cheek teeth, the incisors and the left cheek teeth. At 16 dpf, we observed the
290 budding of the dental lamina with a high condensation of mesenchyme around it. At this
291 stage, it is still impossible to name the teeth, the epithelium being continuous in thickness and
292 shape over the entire length of the bud, we never detect individual tooth buds. In the upper
293 jaw, the budding tooth row is rounded, following the vestibular commissure, and measures
294 1.3mm long from the mesial to distal part of the bud (Fig.4). In the lower jaw, the budding
295 tooth row is straighter and smaller with only 0.8 mm long (Fig.5).

296

297 From 18 dpf on, we can identify the teeth and so we will now describe the
298 development of each tooth individually. Rabbit cheek teeth have a thin and long dental stalk
299 compared to the mouse or the fruit bat (Dosedřlová et al., 2015; Popa et al., 2016). We
300 observed that the development of the dP₄ is the fastest, followed by the dP₃, dP₃ and dP₄ that

301 are synchronous and then by the dP^2 so we described tooth development following these
302 categories. For the molars, the M1 is the first to develop and then the development timing
303 follows the mesio-distal organization plan. The lower molar begins their development before
304 the upper molar.

305

306 dP^2 - P^2

307 At 18 dpf, the dP^2 is at a transition stage between bud and cap (Fig.4). The tooth is
308 connected to the oral epithelium and to the followed tooth by the interdental lamina. At the
309 mesial part of the dP^2 , the interdental lamina is present in almost all the diastema length with
310 an oral epithelium link only in the mesial and distal extremities. At 20 dpf, the dP^2 is in a cap
311 stage. The interdental lamina at the mesial part has disappeared but is still present in the distal
312 part of the dP^2 . The dental lamina stalk begin to detach from the oral epithelium. At 22 dpf,
313 the dP^2 is in a bell stage. Initiation of the replacement begins with an epithelial bud from the
314 dental lamina in the lingual part of the dP^2 , called the replacement dental lamina (also named
315 successional lamina). At 24 dpf, the dP^2 is completely detached from the oral epithelium. The
316 replacement dental lamina, still connected to the dP^2 , plunges into the mesenchyme by
317 keeping a lingual orientation (Fig.4). The interdental lamina is now very thin but still connects
318 the replacement dental lamina of the dP^2 to the replacement dental lamina of the dP^3 . At 26
319 dpf, the dP^2 begins its mineralization. The dental replacement lamina of the dP^2 is still
320 growing in a lingual direction. At 28 dpf, the dP^2 have the crown completely mineralized and
321 just begins to mineralize at the root level. The P^2 is in a cap stage and is localized in a disto-
322 lingual plane compared to the dP^2 . At birth, the dP^2 is completely mineralized from the
323 occlusal surface to the roots and the P^2 is still in a cap stage. Four days later, the P^2 is now at
324 the bell stage and begins to move from its lingual position to apical to the dP^2 . Then, around 1
325 month old, the rooted dP^2 is pushed by the P^2 (Fig.2, B). The dP^2 has a completely worn

326 crown surface and the roots begin to reduce, the P² is ready to erupt. P² is hypselodont (with
327 an unlimited growth) whereas the dP² was hypsodont. In adult, the P² display a complex shape
328 with numerous folds filled with cementum at the mesial part of the tooth.

329

330 dP³-P³ / dP₃-P₃ / dP⁴-P⁴

331 At 18 dpf, the dP₃, dP³ and dP⁴ are at the cap stage. The teeth are linked to the oral
332 epithelium and connected to each other with the interdental lamina (Fig.4). At 20 dpf, the dP₃,
333 dP³ and dP⁴ are in a bell stage (Figs.4, 5). Initiation of the replacement begins in the lingual
334 part of the teeth; we detected the replacement dental laminas. The tooth replacement begins in
335 the dP⁴ and we observed a shift in the initiation of replacement with a gradient of
336 development from the distal premolar towards the most mesial premolar. The interdental
337 lamina continues to link all the teeth together but the dental lamina begins to be detached
338 from the oral epithelium. At 22 dpf, the dP³, dP₃ and dP⁴ are at the bell stage. All the
339 premolars display a replacement dental lamina in the lingual side, and in the dP⁴, we can see
340 that this dental lamina begins to dive in the mesio-lingual direction. Each upper and lower
341 tooth is still connected to the others but dental lamina is completely detached from the oral
342 epithelium. At 24 dpf, the premolars have finished their morphogenesis and now mineralize
343 by secreting dentin and enamel. The replacement dental laminas are highly invaginated into
344 the mesenchyme and are still attached to some elements of the interdental laminas. The
345 replacement dental laminas from the dP³ and dP⁴ grow in a mesial orientation whereas the
346 replacement dental lamina of the dP₃ grows towards the base of the deciduous tooth while
347 maintaining its lingual orientation. The interdental lamina is resorbed around the dP₃,
348 detached of the dP³, broken between the dP³ and the dP⁴, and very thin between the other
349 upper teeth. At 26 dpf, the deciduous premolars are now highly mineralized in their occlusal
350 surface. The replacement dental laminas are budding to give the replacement teeth. The P₃ is

351 developing at the lingual basis of the dP₃, the P³ in a mesio-distal plane of the dP³ and the P⁴
352 in a mesio-lingual plane of the dP⁴. At 28 dpf, the dP₃, dP³ and dP⁴ are mineralized to the
353 roots. The permanent premolars are all in the cap stage, localized at the basis of the deciduous
354 teeth in different positions: The P₃ is localized at the basis of the dP₃ in the lingual side, the P³
355 is in a mesio-vestibular plane compared to the dP³ and the P⁴ is in a mesio-lingual plane
356 compared to the dP⁴. At birth, the deciduous premolars are well mineralized with dentin,
357 enamel and cementum. The P₃, P³ and P⁴ are in a bell stage. The P₃ begins to migrate from its
358 lingual position to under the dP₃ whereas P³ and P⁴ are still in their developing position. At 2
359 dpn, the P⁴ begins to mineralize followed two days later by the P₃ and P³. These permanent
360 premolars are now positioned under their deciduous teeth (Fig.2, B, C, Fig.S1). Then, around
361 1 month old, the rooted deciduous teeth dP₃, dP³ and dP⁴ are pushed by the permanent
362 premolars (Fig.2, B). The deciduous premolars have a completely worn crown surface and the
363 roots begin to reduce, the permanent teeth are ready to erupt. All the permanent cheek teeth
364 are hypselodont. In adult, the P³ and P⁴ have a molarized bilophodont shape with a lingual
365 fold filled with cementum, whereas the P₃ has a complex shape with more folds at the mesial
366 part of the tooth (Fig.2, B, C).

367

368 dP₄-P₄

369 At 18 dpf, the dP⁴ is at the cap stage. The dP₄ is connected to the oral epithelium and
370 to the other teeth of the row by the interdental lamina (Fig.5). 2 days later, the dP₄ is at the
371 bell stage and the initiation of the replacement has begun at the lingual part of the tooth,
372 where we detect the replacement dental lamina. At 22 dpf, the dP₄ is the first cheek tooth to
373 mineralize. The tooth is detached from the oral epithelium, but the replacement dental lamina
374 is still connected to the deciduous tooth. At 24 dpf, the replacement dental lamina is detached
375 from the dP₄ that is detached to the other teeth. The replacement dental lamina plunges into

376 the mesenchyme keeping the lingual orientation. At 26 dpf, the P₄ is budding from the
377 replacement dental lamina at the lingual basis of the dP₄ crown. At 28 dpf, the dP₄ is
378 completely mineralized and the P₄ is at the cap stage, localized at the basis of the dP₄ in the
379 lingual side. At birth, the P₄ is the first permanent cheek tooth to mineralize and begins to
380 migrate from its lingual position to below the fully mineralized dP₄. Two days later the
381 permanent tooth is well-localized below the dP₄. At 4 dpn, the dP₄ is the first cheek tooth to
382 erupt (Fig.2, C). Then, around 1 month old, the dP₄ has a completely worn crown surface and
383 the roots begin to reduce, the P₄ is ready to erupt. P₄ is hypselodont with a continuous growth.
384 In adult, the P₄ has a molarized bilophodont shape (Fig.2, C).

385

386 M₁-M¹

387 At 18 dpf, the M₁ is in a bud to cap stage transition and the M¹ in a bud stage (Figs.4,
388 5). At 20 dpf, the M₁ and M¹ are in a cap stage. At 22 dpf, the M₁ is at the early bell stage and
389 the M¹ is in the cap stage. We observed an epithelial bud at the lingual part of the M₁ and M¹,
390 indicating a transient rudimentary successional lamina. At 24 dpf, The M¹ and M₁ are in a bell
391 stage and the lingual buds are no more visible. Molars are connected distally to the M² and M₂
392 but only the M¹ is still connected to a premolar mesially. At 26 dpf, the M₁ begins its
393 mineralization and the M¹ finishes its morphogenesis. At 28 dpf, the M₁ and M¹ have the
394 crown completely mineralized, with dentin, enamel and cementum. Then, in juveniles and
395 adults, we observed that the molars are hypselodont with a bilophodont shape (Fig.2, B, C).

396

397 M₂-M²

398 At 22 dpf, we observed the budding of the continual lamina at the distal part of the
399 tooth row that will give the M² and M₂ by serial addition of molars (Figs.4, 5). At 24 dpf, the
400 M₂ and M² are in a cap stage, and these teeth are still attached mesially to the interdental

401 dental lamina. At 26 dpf, the M_2 and M^2 are in the cap stage and are the only teeth connected
402 with the remains of dental and interdental lamina. At 28 dpf, the M_2 is now detached from the
403 dental lamina and is in a bell stage. The M^2 , in cap stage, is still linked to the dental lamina.
404 At birth, the M_2 begins to mineralize its occlusal surface whereas the M^2 is in bell stage. At 2
405 dpn, the M^2 and M_2 are mineralizing with dentin, enamel and cementum (Fig.2, B, C). Then,
406 in juveniles and adults, we observed that the molars are hypselodont with a bilophodont
407 shape.

408

409 M_3 - M^3

410 At 28 dpf, we observed a completely separated dental lamina that is budding in the
411 distal part of the lower tooth row that will give the M_3 (Fig.5). In the upper row, we also
412 detect the budding of the dental lamina in the distal part of the M^2 that will give the M^3
413 (Fig.4). At 2 dpn, the M_3 is at the cap stage, followed two days later by the M^3 . Then, in a
414 juvenile around 1 month old, we observed that the M^3 is well mineralized but not erupted
415 (Fig.2, B). In adult, the M_3 and M^3 are highly reduced compared to other molars. Among 188
416 observed adult *Oryctolagus cuniculus* specimens, two lacked the upper third molars with no
417 sign of loss, indicating that this tooth can sometimes not be fully developed.

418

419 To summarize, the development of the maxillary teeth is late compared to the
420 mandible counterparts and all the teeth of a same row are not synchronized. In the upper and
421 lower rows, the dP4 is the first forming tooth, that will be followed by the dP3, and then, only
422 in the maxillary, by the dP² (Fig.7). The development of replacement teeth follows the same
423 order. Regarding the molars, the M_1 is the first to develop, followed by the M_2 and finally the
424 M_3 .

425

426
427
428
429
430
431
432
433
434
435
436
437
438
439
440
441
442
443
444
445
446
447
448
449
450

Discussion

We show here the morphology (Fig.6) and the chronology of rabbit teeth development(Fig.7). Using 3D reconstructions, we were able to clearly identify the different steps of tooth development and replacement. Our study contains more developmental stages and we separated the results for each tooth, allowing us to obtain a complete and more precise chronology than the ones available in the literature (Hirschfeld et al., 1973; Michaeli et al., 1980; Navarro et al., 1975; Ooë, 1980). 3D-reconstructions from the placode stage lead to the conclusion that the canine and first premolars dP^1 and dP_{1-2} are never detected in rabbit embryos. These results suggest a complete loss of these teeth in rabbits, contrary to vestigial tooth rudiments in mice (homologous to the dP_3 and dP_4), detected in early tooth development (Sadier et al., 2019; Viriot, Peterková, Peterka, & Lesot, 2002). However, some observations still need to be clarified, as the epithelium link between the vestigial incisor dI^1 and the dI^2 . This relationship was already problematic for Ooë (1980), who discussed the localization of the dI^2 compared to the dI^1 . In mammals, replacement teeth begin their development at the lingual part the deciduous predecessor (Järvinen et al., 2009). Here the dI^1 and dI^2 incisors are in a mesio-distal plan and not in a vestibulo-lingual plan, so it seems more similar to serial development with an interdental lamina between deciduous incisors. However, the rabbit dI^2 has the specificity of being the only tooth to be deciduous and ever growing. For other teeth, the ever-growing ability appears only in permanent teeth. Hirschfeld et al. (1973) concluded that due to its ever-growing capacity the so-called dI^2 is the permanent tooth coming from the dI^1 . More data on the precise dynamics of the tooth development between 16 and 18 dpf are needed to fully understand the nature of the so-called dI^2 . Reconstructions of the concerned structures during the transition from bud to separated teeth in 3D should help to conclude on the links between these incisors.

451 One particularity of incisor development in rabbits is the appearance of holes that
452 occur only in newborns. The cause of these holes is unknown. These tooth defects have been
453 observed in all our samples, indicating a common phenomenon. We did not find in literature
454 any description of systematic presence of tooth defects at one specific age in rabbits or other
455 species. In this study, we worked on common rabbit breeding regularly crossed with wild
456 rabbits to ensure genetic mixing, limiting the possibility that these dental abnormalities are
457 specific to one genetic selection in a closed breeding. Some hypotheses can be considered to
458 explain the hole formation, as a possible mechanical compression due to the development of
459 adjacent teeth or bone mineralization or the result of molecular signals. It could be interesting
460 to identify which mechanical forces at birth could be responsible for tooth fractures without
461 morphologically affecting the other tissues. These causes could be purely mechanical
462 (development of the bones or the other upper incisors) or molecularly facilitated (involvement
463 of signaling pathways involved in root resorption for example). The observed reparation
464 system, which systematically takes place in the first days of an animal's life, indicates an
465 ability of quick tooth repair, probably due to the high secretion capacity of the odontoblasts in
466 the ever-growing incisor. This speed in tooth repair is incompatible with the classical
467 reparative dentin that require differentiation and migration of new odontoblasts from a pulpal
468 progenitor cell (Moses, Butler, & Qin, 2006). So here, another type of tertiary dentin could
469 close the hole, the reactionary dentin that is formed from a pre-existing odontoblast.

470

471 The 3D-reconstructions of the rabbit premolars indicate that the permanent upper
472 premolar begins its morphogenesis in a mesio-vestibular plane compared to its deciduous
473 tooth, so in the opposite side in contrast to the other teeth. Popa et al. (2016) presented in the
474 fruit bat different modalities of tooth replacement throughout the jaw. They showed, using
475 3D-reconstructions, that the canine, the second and the third premolar do not have the same

476 modalities of replacement due to the relative position of the deciduous and permanent teeth.
477 In rabbit, the initiation of the tooth replacement always begins by a growth of the dental
478 lamina at the lingual position of the tooth that will give the replacement dental lamina as in
479 the ferret or fruit bat (Jussila et al., 2014, Popa et al., 2016). Then, the separation between the
480 first generation of teeth, the oral epithelium and the replacement dental lamina can vary. First,
481 the teeth lose their connection with the oral epithelium. Variations are then observed; the
482 replacement dental lamina can first be separated from the tooth or from the interdental lamina.
483 Concerning the tooth position of the second generation compared to the first it also depends
484 on the teeth as in the fruit bat. For the lower premolars and the upper incisor, the permanent
485 teeth develop directly on the lingual side of the deciduous teeth. For the upper cheek teeth, the
486 position of the second-generation development varies for each premolar. The tooth
487 replacement begins at the lingual part of the deciduous tooth, but then the replacement dental
488 lamina plunges and develops in different orientation depending on the tooth. The P² is
489 localized in a disto-lingual plane compared to the dP², the P³ is in a mesio-vestibular plane
490 compared to the dP³ and the P⁴ is in a mesio-lingual plane compared to the dP⁴. Indeed, the P²
491 and P³ develop on the same frontal plan, with one lingualy and the other vestibulary. Then, all
492 the permanent teeth migrate under the associated deciduous teeth. Compared to the fruit bat or
493 the ferret (Järvinen et al., 2009; Popa et al., 2016), the rabbit dental replacement lamina seems
494 to plunge much deeper into the mesenchyme before it begins to initiate its permanent tooth
495 morphogenesis, as observed in the minipig (Wang et al. 2014).

496

497 During rabbit molar development, we observed buddings at the lingual part of the first
498 molars that quickly disappear. Same tooth shape has been observed in the mouse; a
499 rudimentary successional dental lamina (RSDL) is visible in the lingual part of the M₁ tooth
500 germ (Dosedělová et al., 2015). The RSDL in mouse as in the rabbit does not have

501 odontogenic potential (Popa, Buchtova, & Tucker, 2019). However, by stabilizing the Wnt/ β -
502 catenin signaling in the RSDL, it is possible to obtain a new tooth (Popa et al., 2019). The
503 molars can be considered as deciduous teeth that are never replaced (Luckett, 1993); the study
504 of this budding observed in the rabbit with the molecular information obtained in mutant mice
505 could identify why these teeth are not replaced.

506

507 In this study, we have shown that the rabbit seem to be a good model in dental
508 research. Rabbits are already used in odontological studies but we showed here that they are
509 also useful for studying tooth morphogenesis. Studies of tooth development and replacement
510 in rabbits could allow understanding the mechanisms of mammalian tooth replacement. We
511 showed that common molecular experiments can be done in rabbit tissues as *in situ*
512 hybridization and rabbits can also be a relevant model to use more advanced techniques as
513 CRISPR/Cas9 technology (Yan et al., 2014). Compared to other species used to study tooth
514 replacement (the ferret, the fruit bat, the shrew and the minipig), rabbit embryos are easy to
515 get, with large litters of embryos and a pretty short gestation time (31 days). The main
516 disadvantage to the study of the rabbit compared to the other models already proposed is an
517 incomplete dentition with the lack of the canines. However, rabbits have also ever-growing
518 permanent teeth, allowing study of other issues such as dental stem cells maintaining in
519 addition to mammalian dental replacement.

520

521 **Conclusion**

522 We provided here the description of the complete histo-morphological chronology of
523 the tooth development and replacement in rabbit. It can be considered as a new dataset that
524 allows a better understanding of the dental replacement among mammals. The 3D-
525 reconstructions gave useful information about the geometric organization of the dental

526 replacement and the precise knowledge of the dental development and replacement
527 chronology in this species is a starting point that will allow further studies of gene functions at
528 specific time windows.

529

530 **Acknowledgements**

531 We thank Nicolas Goudemand and all the members of his team for their help and
532 support. We thank all the members of the “Evolution of vertebrate dentition” for the helpful
533 advices and comments. We thank Joanne Burden for help in the final preparation of the
534 manuscript. We thank Cécile Callou, who is responsible for the collection of the lagomorphs
535 at the Museum National d’Histoire Naturelle (MNHN) of Paris, for giving us access to these
536 collections and for her help during our visit. We are grateful to Mathilde Bouchet-Combe,
537 from the SFR Biosciences (UMS3444/CNRS, US8/Inserm, ENSL, UCBL1), who helped for
538 X-Ray microtomographic analyses. The authors declare no conflict of interest

539

540 **Author contributions**

541 L.B.B: contributed to design, to acquisition, analysis, and interpretation, drafted manuscript.
542 L.V: contributed to conception, to analysis and interpretation, critically revised manuscript.
543 T.J: contributed to interpretation, critically revised manuscript. C.C: contributed to conception
544 and design, to analysis and interpretation, critically revised manuscript.

545

546 **References**

547 Balic, A., & Thesleff, I. (2015). Tissue Interactions Regulating Tooth Development and
548 Renewal. *Current Topics in Developmental Biology*, 115, 157–186.
549 <https://doi.org/10.1016/BS.CTDB.2015.07.006>
550 Bertin, T. J. C., Thivichon-Prince, B., LeBlanc, A. R. H., Caldwell, M. W., & Viriot, L.

551 (2018). Current perspectives on tooth implantation, attachment, and replacement in
552 amniota. *Frontiers in Physiology*. Frontiers. <https://doi.org/10.3389/fphys.2018.01630>

553 Bertonnier-Brouty, L., Viriot, L., Joly, T., & Charles, C. (2019). 3D reconstructions of dental
554 epithelium during *Oryctolagus cuniculus* embryonic development related to the
555 publication "Morphological features of tooth development and replacement in the rabbit
556 *Oryctolagus cuniculus*". *MorphoMuseum*, 5:e90. <https://doi.org/10.18563/journal.m3.90>

557 Bosze, Z., & Houdebine, L. M. (2006). Application of rabbits in biomedical research: a
558 review. *World Rabbit Science*, 14(1), 01-14. <https://doi.org/10.4995/wrs.2006.712>

559 Dosedřlová, H., Dumková, J., Lesot, H., Glocová, K., Kunová, M., Tucker, A. S., ...
560 Buchtová, M. (2015). Fate of the molar dental lamina in the monophyodont mouse. *PLoS*
561 *One*, 10(5), e0127543. <https://doi.org/10.1371/journal.pone.0127543>

562 Hirschfeld, Z., Weinreb, M. M., & Michaeli, Y. (1973). Incisors of the Rabbit: Morphology,
563 Histology, and Development. *Journal of Dental Research*, 52(2), 377–384.
564 <https://doi.org/10.1177/00220345730520023201>

565 Horowitz, S. L., Weisbroth, S. H., & Scher, S. (1973). Deciduous dentition in the rabbit
566 (*Oryctolagus cuniculus*). A roentgenographic study. *Archives of Oral Biology*, 18(4),
567 517–523.

568 Järvinen, E., Tummers, M., & Thesleff, I. (2009). The role of the dental lamina in mammalian
569 tooth replacement. *Journal of Experimental Zoology Part B: Molecular and*
570 *Developmental Evolution*, 312B(4), 281–291. <https://doi.org/10.1002/jez.b.21275>

571 Järvinen, E., Välimäki, K., Pummila, M., Thesleff, I., & Jernvall, J. (2008). The taming of the
572 shrew milk teeth. *Evolution and Development*, 10(4), 477–486.
573 <https://doi.org/10.1111/j.1525-142X.2008.00258.x>

574 Jussila, M., Crespo Yanez, X., & Thesleff, I. (2014). Initiation of teeth from the dental lamina
575 in the ferret. *Differentiation*, 87(1), 32–43. <https://doi.org/10.1016/j.diff.2013.11.004>

576 Juuri, E., & Balic, A. (2017). The Biology Underlying Abnormalities of Tooth Number in
577 Humans. *Journal of Dental Research*, *96*(11), 1248–1256.
578 <https://doi.org/10.1177/0022034517720158>

579 Lockett, W. P. (1993). An Ontogenetic Assessment of Dental Homologies in Therian
580 Mammals. In *Mammal Phylogeny* (pp. 182–204). New York, NY.
581 https://doi.org/10.1007/978-1-4615-7381-4_13

582 Metscher, B. D. (2009). MicroCT for comparative morphology: simple staining methods
583 allow high-contrast 3D imaging of diverse non-mineralized animal tissues. *BMC*
584 *Physiology*, *9*, 11. <https://doi.org/10.1186/1472-6793-9-11>

585 Michaeli, Y., Hirschfeld, Z., & Weinreb, M. M. (1980). The cheek teeth of the rabbit:
586 morphology, histology and development. *Cells Tissues Organs*, *106*(2), 223–239.
587 <https://doi.org/10.1159/000145185>

588 Moses, K. D., Butler, W. T., & Qin, C. (2006). Immunohistochemical study of small integrin-
589 binding ligand, N-linked glycoproteins in reactionary dentin of rat molars at different
590 ages. *European Journal of Oral Sciences*, *114*(3), 216–222.
591 <https://doi.org/10.1111/j.1600-0722.2006.00353.x>

592 Mucchielli, M. L., & Mitsiadis, T. A. (2000). Correlation of asymmetric Notch2 expression
593 and mouse incisor rotation. *Mechanisms of Development*, *91*(1–2), 379–382.
594 [https://doi.org/10.1016/S0925-4773\(99\)00293-2](https://doi.org/10.1016/S0925-4773(99)00293-2)

595 Navarro, J. A. C., Sottovia-Filho, D., Leite-Ribeiro, M. C., & Taga, R. (1975). Histological
596 Study on the Postnatal Development and Sequence of Eruption of the Maxillary Cheek-
597 Teeth of Rabbits (*Oryctolagus cuniculus*). *Archivum Histologicum Japonicum*, *38*(1),
598 17–30. <https://doi.org/10.1679/aohc1950.38.17>

599 Navarro, J. A. C., Sottovia-Filho, D., Leite-Ribeiro, M. C., & Taga, R. (1976). Histological
600 study on the postnatal development and sequence of eruption of the mandibular cheek-

601 teeth of rabbits (*Oryctolagus cuniculus*). *Archivum Histologicum Japonicum. Nippon*
602 *Soshikigaku Kiroku*, 39(1), 23–32. <https://doi.org/10.1679/aohc1950.39.23>

603 Ooë, T. (1980). Développement embryonnaire des incisives chez le lapin (*Oryctolagus*
604 *cuniculus* L.). Interpretation de la formule dentaire. *Mammalia*, 44(2), 259–270.
605 <https://doi.org/10.1515/mamm.1980.44.2.259>

606 Popa, E. M., Anthwal, N., & Tucker, A. S. (2016). Complex patterns of tooth replacement
607 revealed in the fruit bat (*Eidolon helvum*). *Journal of Anatomy*, 229(6), 847–856.
608 <https://doi.org/10.1111/joa.12522>

609 Popa, E. M., Buchtova, M., & Tucker, A. S. (2019). Revitalising the rudimentary replacement
610 dentition in the mouse. *Development*, 146(3), dev171363.
611 <https://doi.org/10.1242/dev.171363>

612 Rasch, L. J., Martin, K. J., Cooper, R. L., Metscher, B. D., Underwood, C. J., & Fraser, G. J.
613 (2016). An ancient dental gene set governs development and continuous regeneration of
614 teeth in sharks. <https://doi.org/10.1016/j.ydbio.2016.01.038>

615 Sadier, A., Twarogowska, M., Steklikova, K., Hayden, L., Lambert, A., Schneider, P., ...
616 Pantalacci, S. (2019). Modeling Edar expression reveals the hidden dynamics of tooth
617 signaling center patterning. *PLOS Biology*, 17(2), e3000064.
618 <https://doi.org/10.1371/journal.pbio.3000064>

619 Sych, L. S., & Reade, P. C. (1987). Heterochrony in the development of vestigial and
620 functional deciduous incisors in rabbits (*Oryctolagus cuniculus* L.). *Journal of*
621 *Craniofacial Genetics and Developmental Biology*, 7(1), 81–94.

622 Tummers, M., & Thesleff, I. (2003). Root or crown: a developmental choice orchestrated by
623 the differential regulation of the epithelial stem cell niche in the tooth of two rodent
624 species. *Development (Cambridge, England)*, 130(6), 1049–1057.
625 <https://doi.org/10.1242/dev.00332>

626 Viriot, L., Peterková, R., Peterka, M., & Lesot, H. (2002). Evolutionary Implications of the
627 Occurrence of Two Vestigial Tooth Germs During Early Odontogenesis in the Mouse
628 Lower Jaw. *Connective Tissue Research*, 43(2–3), 129–133.
629 <https://doi.org/10.1080/03008200290001168>

630 Wang, F., Li, G., Wu, Z., Fan, Z., Yang, M., Wu, T., ... Wang, S. (2019). Tracking
631 diphyodont development in miniature pig in vitro and in vivo. *Biology Open*,
632 bio.037036. <https://doi.org/10.1242/bio.037036>

633 Wang, F., Xiao, J., Cong, W., Li, A., Song, T., Wei, F., ... Wang, S. (2014). Morphology and
634 chronology of diphyodont dentition in miniature pigs, *Sus Scrofa*. *Oral Diseases*, 20(4),
635 367–379. <https://doi.org/10.1111/odi.12126>

636 Whitlock, J. A., & Richman, J. M. (2013). Biology of tooth replacement in amniotes.
637 *International Journal of Oral Science*, 5(2), 66–70. <https://doi.org/10.1038/ijos.2013.36>

638 Yan, Q., Zhang, Q., Yang, H., Zou, Q., Tang, C., Fan, N., & Lai, L. (2014). Generation of
639 multi-gene knockout rabbits using the Cas9/gRNA system. *Cell Regeneration*, 3(1),
640 3:12. <https://doi.org/10.1186/2045-9769-3-12>

641

642

643

644

645

646

647

648

649

650

651 **Figure legends**

652

653 **Fig.1.** 3D-reconstructions of the epithelial part of the upper incisors during development.
654 Development of the dI^1 , dI^2 , dI^3 and I^3 from 14 to 28 days post-fertilization (dpf). Indicated in
655 blue, the vestigial incisor; in pink, the interdental lamina; in black (dotted line), the dental
656 tissues; in black (arrow), the replacement tissues. M, mesial; L, lingual; O, occlusal.

657

658 **Fig.2.** 3D-reconstructions of the mineralized part of the rabbit teeth. (A) Mineralized tissues
659 of the upper incisors from embryo to adult. (B) Mineralized tissues of the upper cheek teeth
660 from newborn to adult. (C) Mineralized tissues of the lower cheek teeth in newborn and adult.
661 (D) Tooth nomenclature: “I”, “P” and “M” for incisor, premolar and molar; the deciduous
662 teeth are indicated with a “d”; the tooth number is in exponent for the upper teeth and in an
663 index for the lower teeth. In blue the vestigial incisor, in red all the deciduous teeth that will
664 be replaced.

665

666 **Fig.3.** Hole repartition in the upper incisor. (A) Distribution of the holes in 10 upper incisors
667 from 0 to 4 days post-natal (dpn). (B) Distribution of the holes in the two dI^2 from a same
668 individual. Each arrow indicates a fold. (C) Histological sections of a hole in a 0 and (D) 4
669 dpn individual. (E) *Osteocalcin* staining and (F) *Keratin 14* staining in a 0 dpn incisor.

670

671 **Fig.4.** 3D-reconstructions of the epithelial tissues and histology in rabbit upper cheek teeth
672 from 14 dpf to 28 dpf. 3D-reconstruction of the epithelial tissues of the upper cheek teeth and
673 frontal sections associated for each tooth. Indicated with the black arrow, the permanent
674 premolars. M, mesial; L, lingual; O, occlusal; D, distal; V, vestibular.

675

676 **Fig.5.** 3D-reconstructions of the epithelial tissues and histology in rabbit lower cheek teeth
677 from 14 dpf to 28 dpf. 3D-reconstruction of the epithelial tissues of the lower cheek teeth and
678 frontal sections associated for each tooth. M, mesial; L, lingual; O, occlusal; D, distal; V,
679 vestibular.

680

681 **Fig.6.** Summary of the dental replacement progression in rabbit. The black triangle shows the
682 initiation of the replacement dental lamina, the black star the separation of the replacement
683 dental lamina and the deciduous tooth and the white triangle the morphogenesis initiation of
684 the permanent tooth. Scale bar: 200 μ m

685

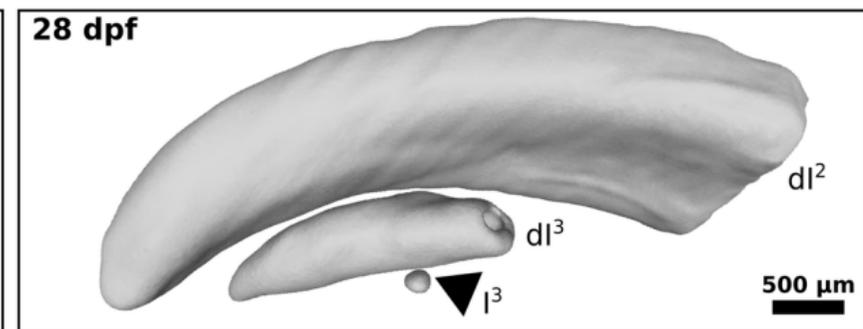
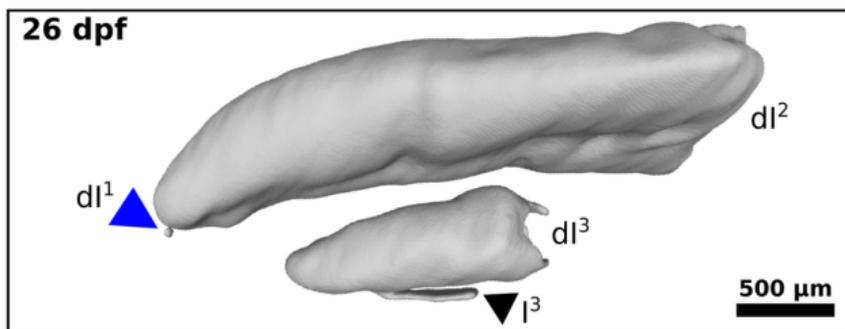
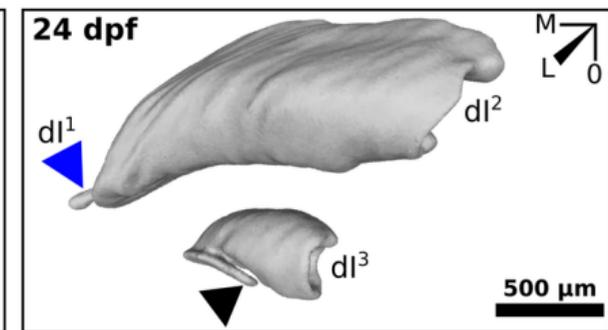
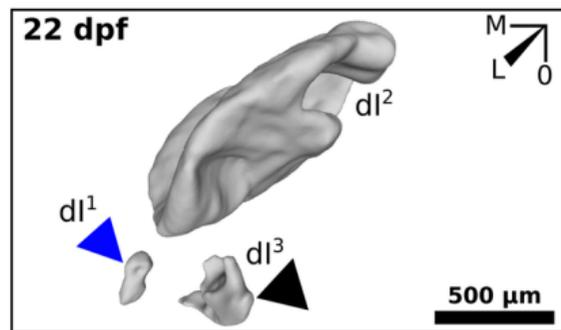
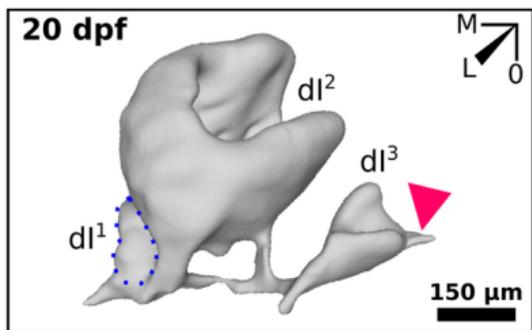
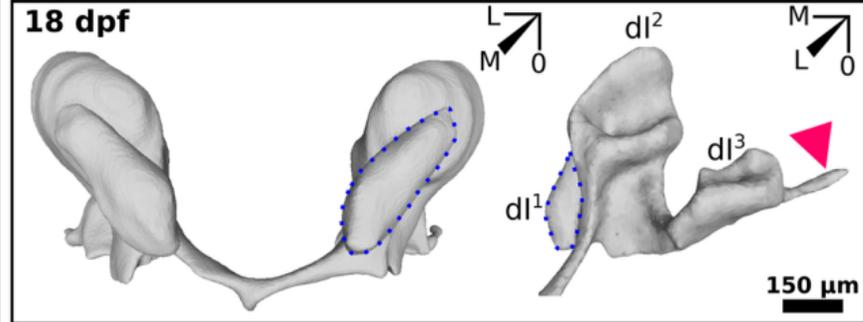
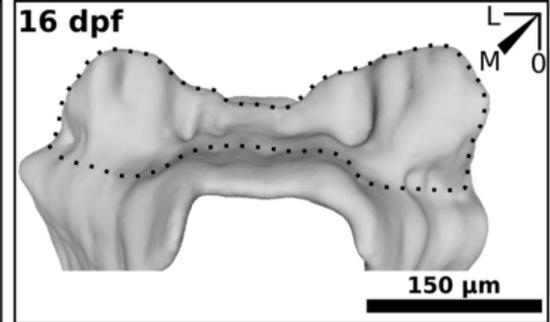
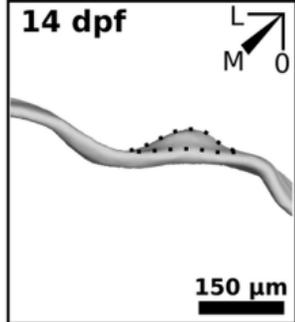
686 **Fig.7.** Chronology of dental development and replacement for each rabbit tooth from 12 dpf
687 to 4 dpn.

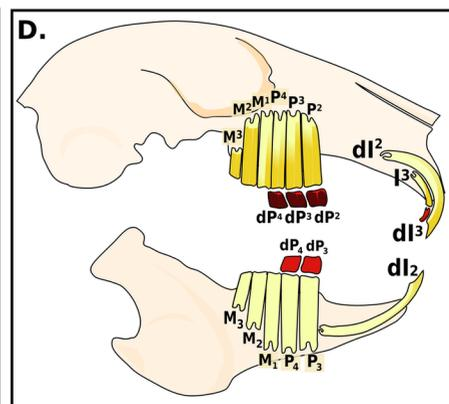
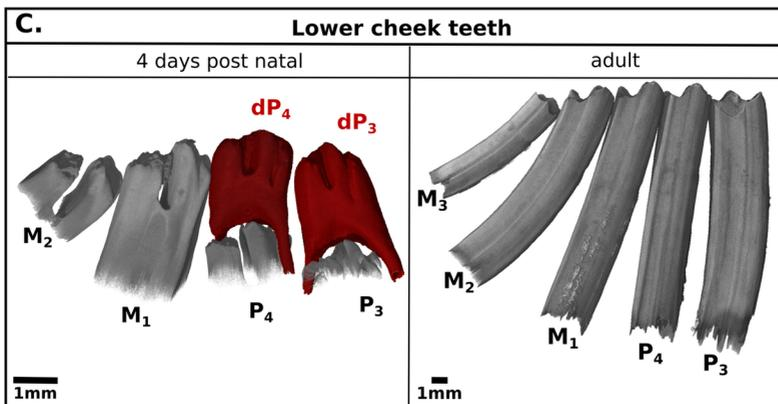
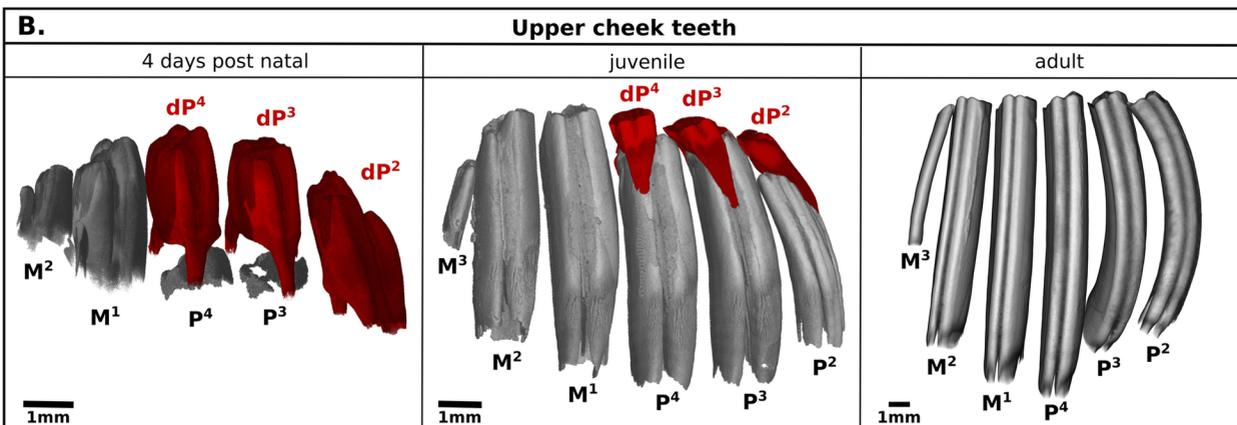
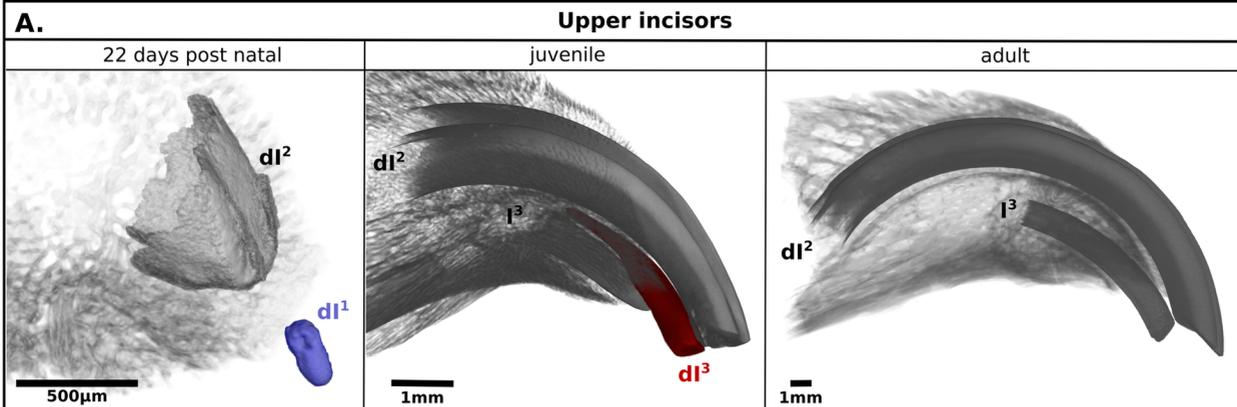
688

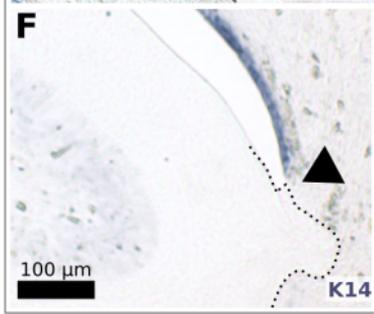
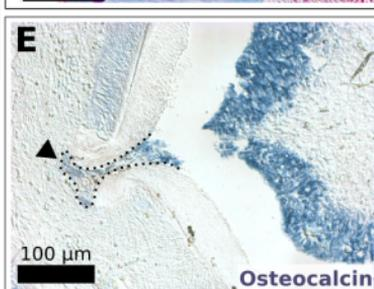
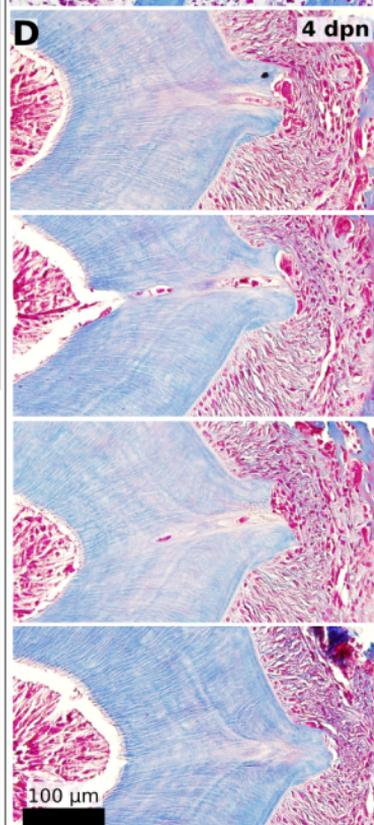
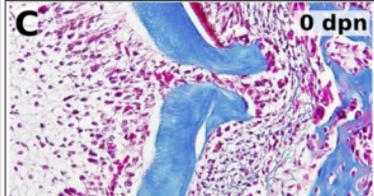
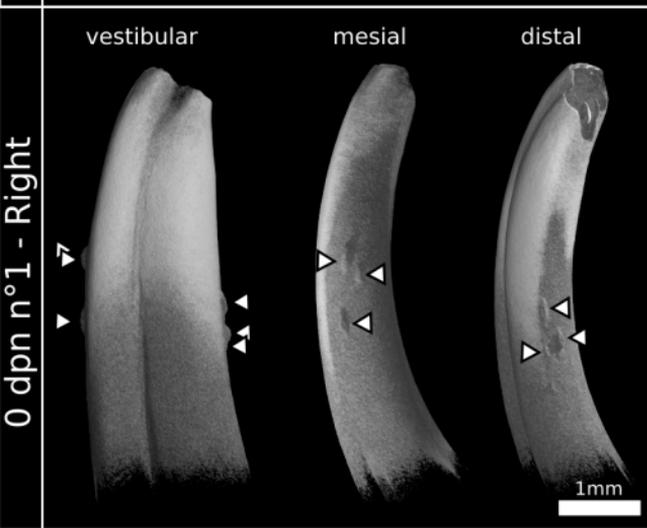
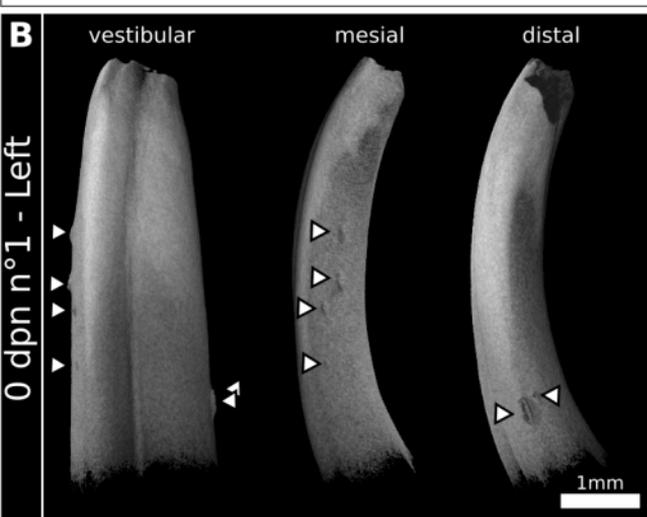
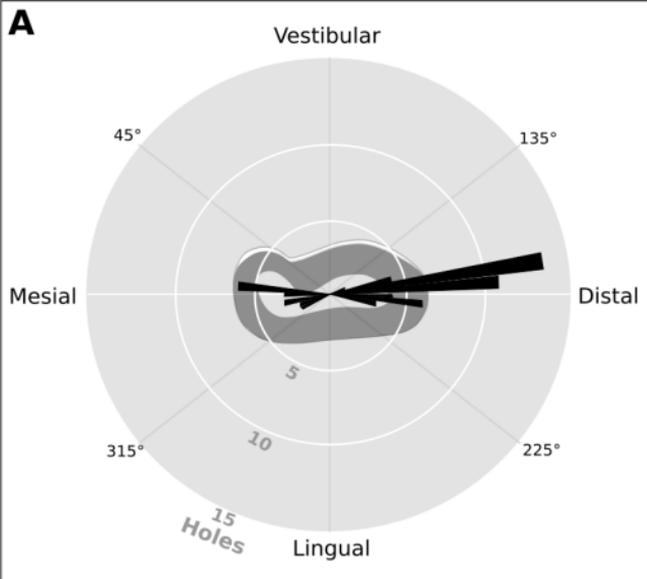
689 **Fig.S1.** Histological sections of the rabbit upper incisors and lower cheek teeth. (A) Frontal
690 and sagittal sections of the upper incisors from 18 dpf to 4 dpn. Indicated with black arrows,
691 the replacement dental lamina. (B) Frontal sections of the lower third premolar from 0 dpn to
692 4 dpn. L, lingual; O, occlusal. Scale bar: 200 μ m.

693

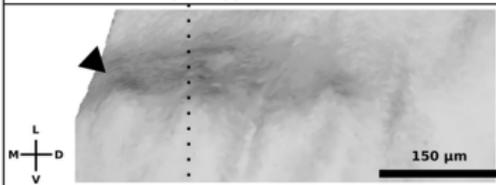
694 **Fig.S2.** Views of the 3D reconstructions of the upper incisors mineralized tissues and virtual
695 sections of the incisors. In sections, the dentin appears in grey and the enamel in white.
696 Indicated in blue, enamel layer in the dI²; in yellow, enamel layer in the dI³; in red, enamel
697 layer in the I³. The white dotted line indicates the frontal section plane illustrated in the white
698 rectangle. V, vestibular; M, mesial. Scale bar: 1mm.



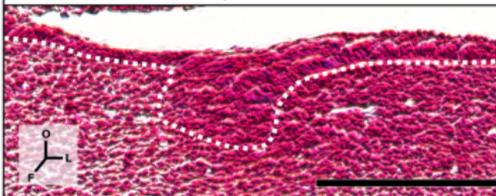




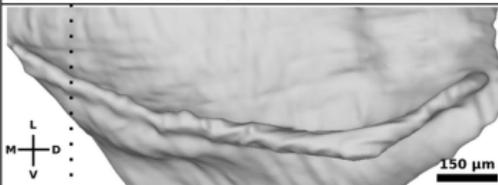
14dpf - Upper cheek teeth



placode



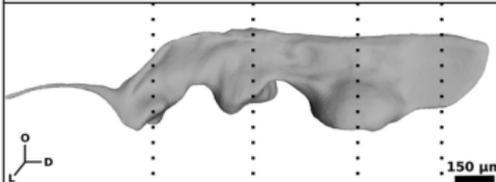
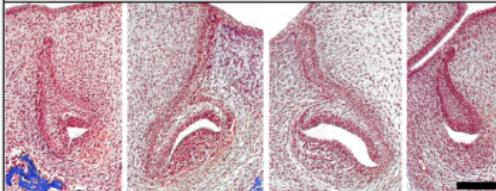
16 dpf - Upper cheek teeth



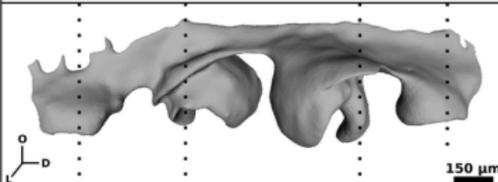
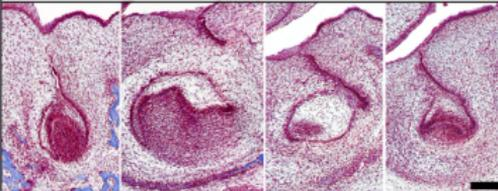
bud



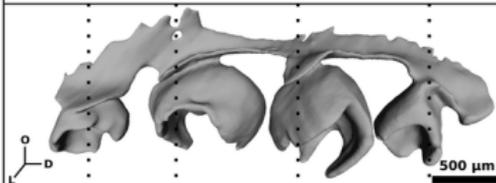
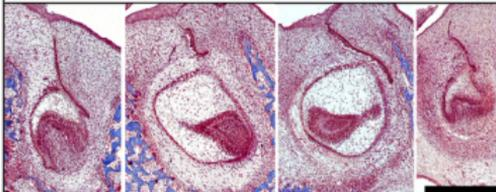
18 dpf - Upper cheek teeth

dP²dP³dP⁴M¹

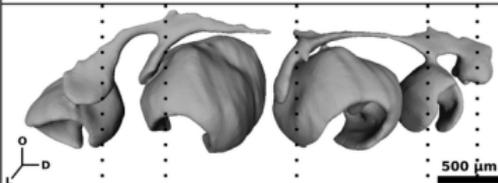
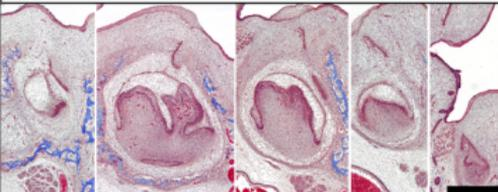
20 dpf - Upper cheek teeth

dP²dP³dP⁴M¹

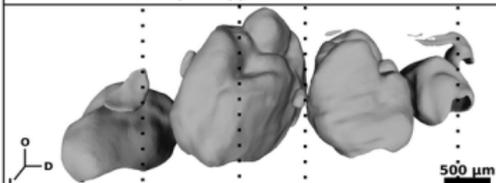
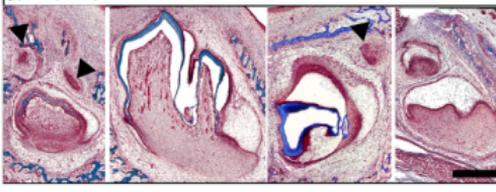
22 dpf - Upper cheek teeth

dP²dP³dP⁴M¹

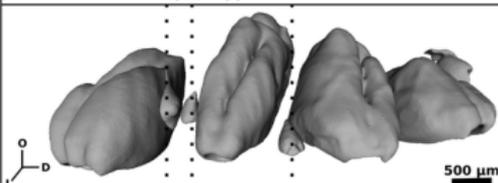
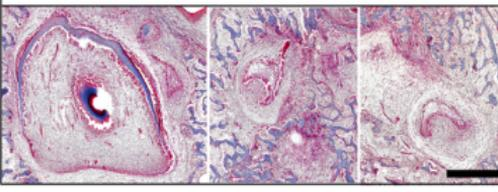
24 dpf - Upper cheek teeth

dP²dP³dP⁴M¹M²

26 dpf - Upper cheek teeth

dP² - P² - P³dP³dP⁴ - P⁴M¹ - M²

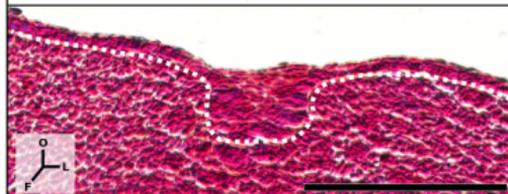
28 dpf - Upper cheek teeth

dP²P³P⁴

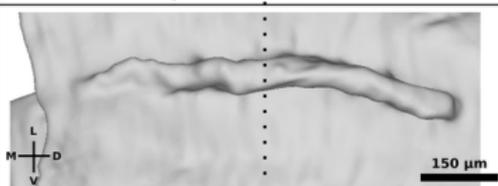
14 dpf - Lower cheek teeth



placode



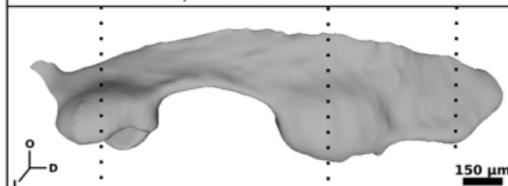
16 dpf - Lower cheek teeth



bud



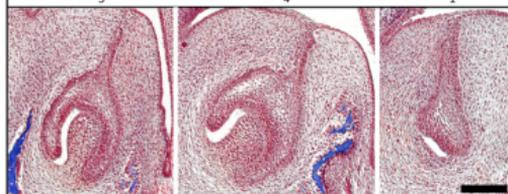
18 dpf - Lower cheek teeth



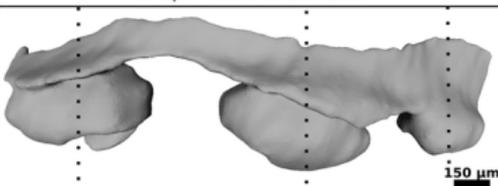
dP₃

dP₄

M₁



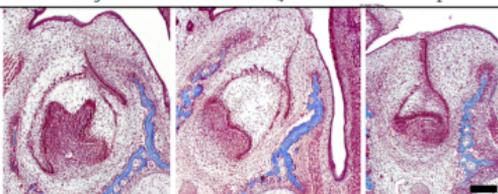
20 dpf - Lower cheek teeth



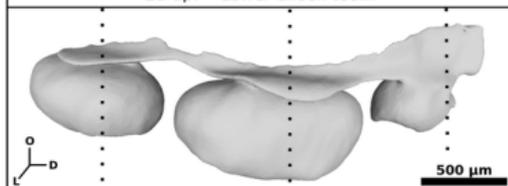
dP₃

dP₄

M₁



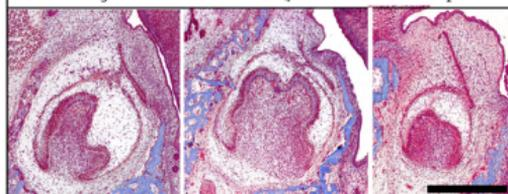
22 dpf - Lower cheek teeth



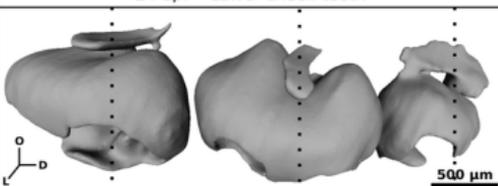
dP₃

dP₄

M₁



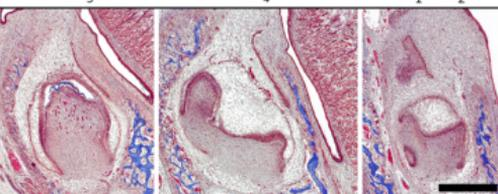
24 dpf - Lower cheek teeth



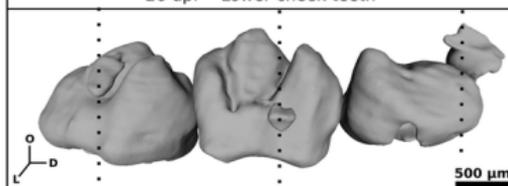
dP₃

dP₄

M₁ - M₂



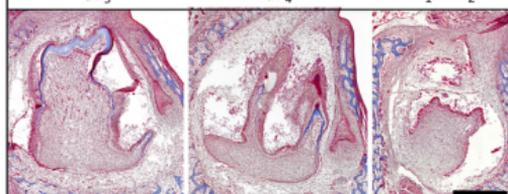
26 dpf - Lower cheek teeth



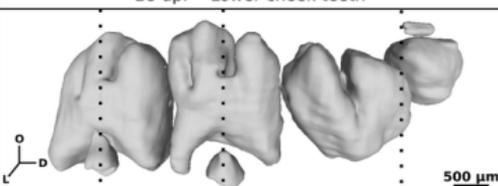
dP₃

dP₄

M₁ - M₂



28 dpf - Lower cheek teeth



dP₃

dP₄

M₁ - M₂

